Did the Eruption of the Mt. Pinatubo Volcano Affect Cirrus Properties?

ZHENGZHAO LUO

Department of Earth and Environmental Sciences, Columbia University, New York, New York

WILLIAM B. ROSSOW

NASA Goddard Institute for Space Studies, New York, New York

TOSHIRO INOUE

Meteorological Research Institute, Tsukuba, Ibaraki, Japan

CLAUDIA J. STUBENRAUCH

Laboratorie de Météorologie Dynamique du CNRS, Ecole Polytechnique, Palaiseau, France

ABSTRACT

Some observations suggest that the volcanic aerosols produced by the Mt. Pinatubo eruption may have altered cirrus. The authors look for evidence that such modification of cirrus is extensive enough to be climatically significant by comparing three satellite-based cirrus datasets produced by the International Satellite Cloud Climatology Project (ISCCP) analysis, the split-window analysis, and the Improved Initialization Inversion (3I) analysis. Since the former two have not been compared in detail before, such a comparison was conducted here. When applied to the Advanced Very High Resolution Radiometer (AVHRR) data, both the ISCCP and split-window analyses identify about 0.2–0.3 cirrus cloud amounts in tropical latitudes; however, there are detailed differences of classification for about half of these clouds. The discrepancies are attributed to the simplified assumptions made by both methods. The latter two datasets are derived from infrared radiances, so they are less sensitive to volcanic aerosols than the ISCCP analysis. After the Mt. Pinatubo eruption, the ISCCP results indicate a notable decrease of thin cirrus over ocean, accompanied by a comparable increase of altocumulus and cumulus clouds; over land, there are no significant changes. In contrast, results from the split-window and 3I analyses show little change in thin cirrus amount over either ocean or land that is associated with the volcanic eruption. The ISCCP results can, therefore, be understood as a misclassification of thin cirrus because additional reflected sunlight by the volcanic aerosol makes the cirrus clouds appear to be optically thicker. Examinations of the split-window signature show no significant change in infrared emissivity (or optical thickness). These results indicate that the Mt. Pinatubo volcanic aerosol did not have a significant systematic effect on tropical cirrus properties (such as cloud amount and optical thickness), but do not exclude the occurrence of temporary, local effects. Hence, these results suggest that there is no significant climate feedback produced by aerosol–cirrus–radiative interactions.

1. Introduction

Cirrus clouds are high level (upper troposphere), optically thin, ice clouds with both low solar reflectivities and low emissivities (Liou 1986). Globally, they cover around 20% of the earth's surface (Rossow and Schiffer 1999), but there may be another 5%–10% of very thin cirrus present (Jin et al. 1996; Liao et al. 1995; Stubenrauch et al. 1999b). Unlike most other clouds, cirrus with cloud tops higher than the effective emission level

of the clear atmosphere cause net radiative heating of the earth–atmosphere system because they reflect sunlight less than they decrease the outgoing longwave radiation. This warming effect is reversed as cirrus cloud optical thickness increases (Stephens et al. 1990). Through their radiative effects cirrus clouds can modulate the general circulation of the atmosphere (Randall et al. 1989; Ramanathan et al. 1983).

There are many ways to observe cirrus properties and behavior; however, only satellites provide the global overview of cloud systems at the scale of the synoptic weather systems in which they form (Rossow 1989). The past two decades have witnessed numerous studies of cirrus clouds using satellite instruments. Inoue (1985)

Corresponding author address: Zhengzhao Luo, Dept. of Earth and Environmental Sciences, Columbia University, 2880 Broadway, Room 608, New York, NY 10025.
E-mail: zluo@giss.nasa.gov

showed the feasibility of cirrus detection using the split-window data (wavelengths around 11 and 12 μm) of the Advanced Very High Resolution Radiometer (AVHRR) on board the National Oceanic and Atmospheric Administration's (NOAA's) satellite *NOAA-7* and derived the temperature and the emissivity of cirrus clouds. Furthermore, based on a threshold technique using two-dimensional brightness temperature histograms, he developed a method that could be used to identify several types of clouds (Inoue 1987). The International Satellite Cloud Climatology Project (ISCCP) was established in 1982 to produce a globally uniform satellite cloud climatology (Schiffer and Rossow 1983; Rossow and Schiffer 1991). In the second version of the cloud product, sensitivity to cirrus is increased and biases in cirrus cloud optical thickness and cloud-top temperature are reduced (Rossow and Schiffer 1999). Wylie et al. (1994) applied the CO_2 slicing technique, which makes use of infrared radiances at wavelengths from 13 to 15 μm from the High Resolution Infrared Radiation Sounder (HIRS) data from NOAA polar-orbiting satellites, to derive four years of high cloud climatology. Their new study extends the climatology to eight years (Wylie and Menzel 1999). More recently, Stubenrauch et al. (1999a) developed a new Improved Initialization Inversion (3I) algorithm and used it to convert the Television Infrared Observational Satellite (TIROS-N) Operational Vertical Sounder (TOVS) observations from NOAA polar-orbiting environmental satellites into atmospheric temperature and water vapor profiles, as well as cloud and surface properties. Cirrus clouds are separated from high opaque clouds by their lower emissivities.

Volcanic activities may alter cirrus properties. Jensen and Toon (1992) suggested the potential effect of volcanic aerosols on cirrus cloud microphysics using simulations, while Sassen (1992) and Sassen et al. (1995) proposed a volcano–cirrus–climate feedback mechanism based on analysis of two days of data from the First ISCCP Regional Experiment (FIRE). Moreover, Song et al. (1996) examined the interannual variability of the high-level cloudiness (HC) index and found a widespread increase of the HC index up to 0.1 after major volcanoes. However, ISCCP results suggest that the production of large amounts of stratospheric aerosol by Mt. Pinatubo is associated with a decrease in cirrus cloud amount by 0.02–0.04 and an increase in their average optical thickness (Rossow and Schiffer 1999). How exactly did Mt. Pinatubo volcano affect cirrus properties? We explore this question by comparing the ISCCP products with two other cloud datasets derived from the split-window method and 3I cloud algorithm (Stubenrauch et al. 1999a).

In the first half of the paper, we report a systematic comparison between cirrus retrieved by ISCCP and the split-window method. This comparison study serves as a preparation for the second half of the paper, which addresses how the Mt. Pinatubo eruption affected cirrus

properties. First, a radiative transfer model is used to analyze the two algorithms, because the split-window method is based on the identification of clusters in multidimensional radiance space, while the ISCCP cloud scheme relies on a radiative transfer model to retrieve cloud properties. Second, retrieved cloud information is compared in light of the model simulation results. Cirrus from the 3I cloud dataset have been compared to those from ISCCP by Stubenrauch et al. (1999b); note also the paper by Jin et al. (1996) that compared ISCCP to the CO_2 slicing analysis of HIRS data.

In the second half of the paper, we make use of the different sensitivities of the three cloud retrieval algorithms to explore the influence of the Mt. Pinatubo volcano eruption on cirrus properties. One major difference between the split-window method, 3I cloud algorithm, and the ISCCP cloud scheme is that the former two use radiances at infrared wavelengths, while the latter utilizes one infrared and one visible radiance. Since absorption in the infrared is less sensitive to aerosols than reflection in the visible, the split-window method and 3I cloud algorithm do a better job of monitoring thin cirrus even when stratospheric aerosol concentration is relatively high, such as after a large volcanic eruption. The ISCCP cloud scheme, which depends on visible reflectance to derive cloud optical thickness, could attribute the additional visible reflectance caused by aerosols to clouds, thus introducing errors in the cloud retrieval (Rossow and Schiffer 1999). Hence, there may be artifacts in the changes of ISCCP-retrieved cirrus after the eruption of the Mt. Pinatubo volcano, whereas cirrus retrieved by the split-window method and 3I cloud algorithm are less likely to be affected by the event.

This paper is divided into five sections. Section 2 gives a short description of the datasets and cloud retrieval techniques used in the study. Section 3 presents a comparison of the split-window and ISCCP cloud algorithms, using both simulations and observations. In section 4, cloud datasets from ISCCP, the split-window method, and 3I are examined to find out the influence of the Mt. Pinatubo eruption on cirrus properties. Section 5 summarizes the main findings.

2. Data and analysis methodologies

a. AVHRR datasets and split-window method

Channel 4 ($\approx$11 μm) and channel 5 ($\approx$12 μm) data from AVHRR on *NOAA-7* were used by Inoue (1987, 1989) to develop his split-window method. In this paper, we continue to use AVHRR data (sampled and saved in the ISCCP DX products) from *NOAA-11* for the period from January 1989 to December 1993, covering both the pre- and posteruption period (the Mt. Pinatubo volcano erupted in June 1991). AVHRR also has two solar channels (wavelengths of 0.6 and 0.7 μm, respectively) and one near the infrared channel (wave-

BTD			
Thick cirrus	Thin cirrus	
Dense cirrus	N type	Clear
Cumulonimbus	Cumulus	

BTD			
Thick cirrus	Thin cirrus	
Dense cirrus	N type	Clear
Cumulonimbus	Cumulus	
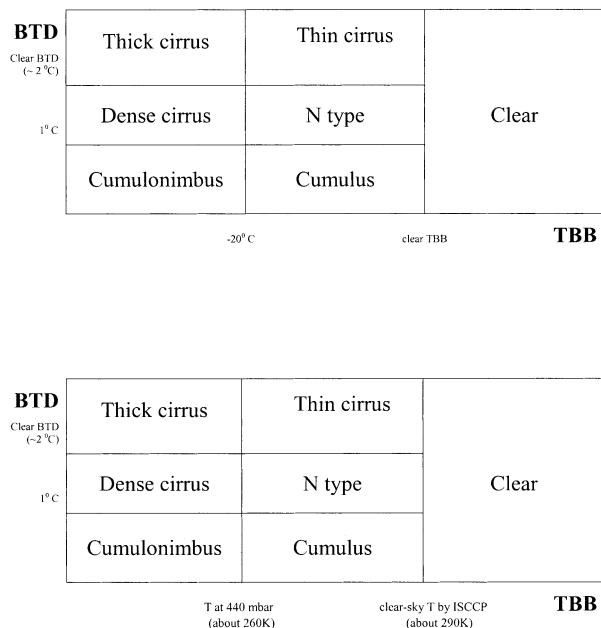
FIG. 1. Cloud classification in the split-window method (Inoue 1989). (a) The original classification algorithm; (b) the modified classification algorithm used in this study.

length of 3.7 μm). The spatial resolution of the global AVHRR product is 4.0 km and the imaging frequency is twice daily at lower latitudes. To save data volume, the ISCCP data is spatially sampled to intervals of approximately 30 km (Schiffer and Rossow 1983).

Inoue (1985) has shown that cirrus clouds can be identified by inspection of the images constructed from the brightness temperature difference (BTD) measured at 11 and 12 μm. In his following papers, Inoue proposed an objective cloud classification method based on a threshold technique in a two-dimensional histogram (Inoue 1987, 1989). Following Inoue (1989), we call this method the split-window method, in which cloud types are classified by the brightness temperature (TBB) at 11 μm and the BTD (11 minus 12 μm) as in Fig. 1a. TBB is used to separate high-level clouds from low-level clouds, while BTD is a good indicator for distinguishing between optically thick and optically thin clouds. The BTD has its lowest value (about zero) for blackbody clouds like cumulonimbus, a moderate value (around 2°C) for clear sky, and the highest value (up to 6°C) for optically thin clouds like cirrus. Clear-sky BTD is due to the spectral dependence of water vapor absorption, while different BTDs for clouds are caused by differences in cloud emissivity.

In this paper, we modify the original classification thresholds of the split-window method in such a way as to facilitate the comparison with the ISCCP data and to take advantage of more information. For example, cloudy or clear in the new version of the split-window method is decided based on the ISCCP cloudy/clear decision. Accordingly, the clear BTD is calculated wher-

ever ISCCP sees clear conditions. This is justified because our main interest is in the comparison of cirrus retrieved by the two cloud schemes and also because the original split-window method utilizes a much simpler threshold test to separate cloudy scenes from clear ones than does ISCCP. Another modification is that the threshold for high-level clouds is changed from a constant TBB ($-20°$C in Fig. 1a) to a variable TBB corresponding to a constant cloud-top pressure, namely, 440 mb (the average temperature at this level in the Tropics and midlatitudes ranges from about $-15°$ to $-25°$C). This is consistent with the cloud classification in the ISCCP cloud scheme (see section 2b). The modified version of cloud classification of the split-window method is shown in Fig. 1b.

b. ISCCP method

ISCCP collects and analyzes infrared ($\approx$11 μm) and visible ($\approx$0.6 μm) radiances measured by the imaging instruments on all the operational weather satellites. In this paper, we only consider the results from *NOAA-11* AVHRR. The ISCCP cloud analysis procedure consists of three principal steps: cloud detection, radiative model analysis, and statistical analysis (Rossow and Schiffer 1991). Cloud detection is achieved in two passes through the whole dataset (Rossow and Garder 1993). First, a series of spatial and temporal tests are performed to estimate clear values of visible and infrared radiances for each field of view (FOV); second, the whole radiance dataset is examined again and each radiance is compared with the corresponding clear value. If either the infrared radiance is smaller than the clear value by more than some threshold amount or the visible radiance is larger than the clear value by more than some threshold amount, the pixel is labeled cloudy. After pixels are classified as clear and cloudy, the measured radiances are compared to radiative transfer model calculations to retrieve cloud-top temperature (Tc) and visible optical thickness (Tau) for cloudy pixels, and surface reflectance and surface temperature for clear pixels. Clouds are represented in the radiative model as a single, thin layer, uniformly covering the image pixel with a specified average particle size and size distribution. When cloud optical thickness is small enough (as for thin cirrus), such that a significant portion of the infrared radiation is transmitted from the surface and atmosphere below, the retrieved value of Tc is reevaluated to account for this transmission. For clouds colder than 260 K, the cloud microphysical model is an ice cloud composed of 30-μm polycrystals (Rossow and Schiffer 1999).

Clouds are classified in ISCCP according to cloud-top pressure (Pc) and optical thickness (Fig. 2). In section 3, simulations employing a radiative transfer model will be used to relate the ISCCP cloud scheme and the split-window method.
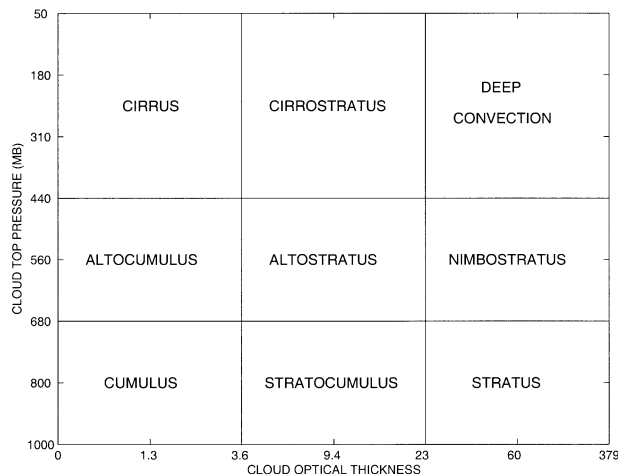
FIG. 2. Cloud classification in the ISCCP D-series datasets.

c. 3I cloud scheme and dataset

The Improved Initialization Inversion (3I) procedure is a physical-statistical algorithm for retrieving atmospheric temperature and water vapor profiles as well as cloud and surface properties from TOVS observations, using HIRS and Microwave Sounding Unit (MSU; Chédin et al. 1985) data. The original 3I cloud scheme was based on a combination of the "CO_2 slicing" method and the "coherence-of-effective-cloud-amount" method, using channels within the CO_2 absorption band around 14 μm (Wahiche et al. 1986; Stubenrauch et al. 1996). Comparison with ISCCP led to an improved 3I cloud retrieval scheme based on a weighted-χ^2 method that estimates the coherence of effective cloud amount at different pressure levels. The introduction of weights that take account of temperature profile uncertainty yields unbiased cloud parameters at all cloud heights for homogeneous cloud types (Stubenrauch et al. 1999a). The 3I cloud properties (cloud-top pressure Pc and effective cloud amount $N\epsilon_{cld}$) are determined from averaged radiances over all cloudy pixels within each 100 km × 100 km box, assuming a single, homogeneous cloud layer. Cirrus are defined as cloud with Pc < 440 mb and $N\epsilon_{cld}$ < 0.9.

Cirrus from the 3I cloud dataset have been compared with those from ISCCP by Stubenrauch et al. (1999b). Results show that 3I identifies 10% more cirrus than ISCCP DX over mid- and low-latitude ocean; over tropical land, the difference is 20%. These discrepancies can be explained in part by the different detection sensitivities for cirrus (cf. Liao et al. 1995; Jin et al. 1996) and in part by small-scale horizontal and vertical heterogeneities to which the two datasets respond differently due to differences in spatial and spectral resolutions (Stubenrauch et al. 1999c).

3. Comparison of cloud retrieval techniques and observations

We present a comparison of the split-window and ISCCP results, since this has not been done before; a detailed comparison of 3I and ISCCP is given in Stubenrauch et al. (1999b,c).

The split-window method is based on the identification of clusters in a two-dimensional brightness temperature histogram of TBB and BTD. The ISCCP cloud analysis relies on a radiative model to retrieve cloud-top pressure (Pc) and cloud optical thickness (Tau) explicitly for each pixel and then uses these properties for a cloud classification. Therefore, a radiative transfer model called Streamer (Key 1996) is used as a bridge to compare these two cloud classifications.

a. Radiative transfer model description

Streamer (version 2.5p) is used to simulate AVHRR split-window channel radiances under clear skies and different cloudy conditions. Streamer can be used for computing either radiances (intensities) or irradiances (fluxes) for any viewing geometry in 24 shortwave and 105 longwave bands under a wide variety of atmospheric and surface conditions. A discrete ordinate solver (Stamnes et al. 1988) is used to compute radiances. Four absorbing gases are considered: water vapor, carbon dioxide, ozone, and oxygen. Seven standard atmospheric profiles are built-in but any other profile can be specified. Cloud optical properties are based on three different parameterization schemes: water cloud scheme (Hu and Stamnes 1993), ice cloud shortwave scheme (Fu and Liou 1993), and ice cloud longwave scheme (parameterized single-scattering properties of ice spheres using Mie theory). Aerosol amounts can be distributed vertically either by a user-supplied profile or one of the built-in standard profiles. In Streamer, "each computation is done for a scene, where the scene can be a mixture of up to 10 cloud types occurring individually, up to 10 overlapping cloud sets of up to 10 clouds each, and the clear sky, all over some combination of up to three surface types" (Key 1996).

Streamer's infrared accuracy in clear-sky conditions has been tested by comparing computations to other models in the Intercomparison of Radiation Codes in Climate Models (ICRCCM; Ellingson et al. 1991). In all five standard cases, ranging from tropical to subarctic winter atmospheres, the longwave fluxes computed by Streamer were within 5% and one standard deviation of the mean of all the models (Jin and Rossow 1997). Pinto et al. (1997) compared Streamer's modeled downwelling broadband longwave irradiance with that of the observation and found a bias of 3 W m^{-2}.

b. Comparison of cloud retrieval techniques

AVHRR radiances from split-window channels are simulated using Streamer for clear skies and different
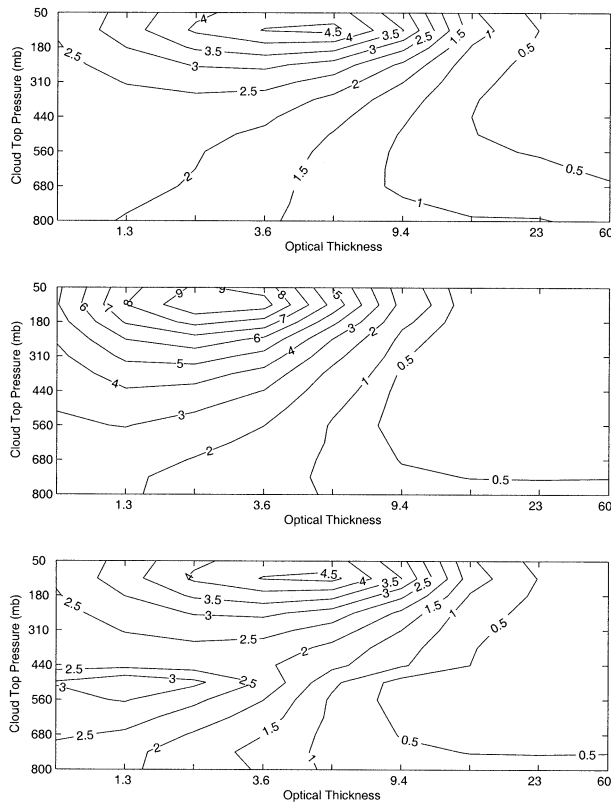
FIG. 3. Simulated satellite (AVHRR) observed BTD for different cloud types as defined in ISCCP (see Fig. 2). (top) Assumption that all clouds are ice clouds; (middle) assumption that all clouds are water clouds; (bottom) combine them by assuming clouds above 440 mb are ice clouds and clouds below are water clouds. Tropical profile is used. Satellite zenith angle is 0° (nadir).

FIG. 4. The same as Fig. 3, except that satellite zenith angle is 60°.

types of clouds represented by their cloud-top pressure (Pc) and optical thickness (Tau) values, consistent with the ISCCP cloud classification (see Fig. 2). Microphysical properties such as cloud particle effective radius (10 μm for water clouds and 30 μm for ice clouds) and water content are specified to be the same as in the ISCCP retrieval model. Since the split-window method makes no explicit assumptions about the microphysics (with one exception noted below), we choose this approach to focus solely on cloud classification differences.

Figures 3 and 4 show a series of simulations of BTD as a function of Pc and Tau for the Air Force Geophysics Laboratory (AFGL) reference tropical profile (McClatchey et al. 1971). Besides Pc and Tau, BTD is also sensitive to cloud phase, cloud particle size distribution, and a few other microphysical properties (Wu 1987; Parol et al. 1991; Giraud et al. 2001). Replacing the single-scattering properties of ice spheres by those of ice polycrystals (Mitchell et al. 1996) in these calculations (not shown) decreases the BTD by about 0.5 K, but the structure of the figure stays the same. The upper panels of the two figures assume all clouds are composed of ice particles, while the middle panels assume

all clouds are water clouds. The lower panels combine these two cases so that clouds above the 440-mb level are ice and clouds below 440 mb are liquid. The simulations are done for two different satellite zenith angles covering the extremes for AVHRR.

Generally, these simulations show that cirrus clouds, which are at high altitude and optically thin, have larger BTD values compared with other clouds and clear sky (BTD is not zero for clear sky because of the spectral dependence of water vapor absorption; see Fig. 5). However, there is one unexpected feature: besides thin cirrus, a second local maximum of BTD exists where Pc is around 500 mb and Tau is about 1.3, depending on satellite zenith angle. This second maximum is caused by two competing effects that combine to determine the BTD values. On the one hand, water clouds have larger BTD values than ice clouds (see Figs. 3 and 4) because BTD tends to be larger for clouds with smaller particle size (Wu 1987; Giraud et al. 2001). On the other hand, BTD also exhibits a larger value for higher and optically thinner clouds, because these clouds (such as cirrus) generate a larger difference in emissivity between the two split-window channels (Inoue 1985). For these reasons, cirrus clouds have larger BTD because they are high and optically thin, while thin liquid altocumulus clouds also have relatively large BTD because they consist of small particles and are also high and thin enough.
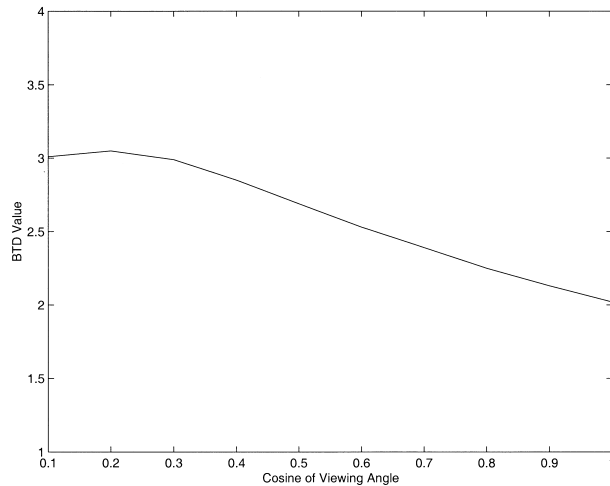
FIG. 5. Simulated satellite (AVHRR) observed clear-sky BTD as a function of satellite zenith angle. Tropical profile is used.

Thus, there is potential for confusion between the thinnest midlevel water clouds and higher-level ice clouds.

In addition to BTD, TBB has also been simulated as a function of P_c and Tau (not shown). Based on the two cloud classification schemes (Figs. 1 and 2) and the simulations of BTD and TBB, we can link the two cloud classifications: Figure 6 shows how clouds classified by ISCCP are categorized by the split-window method, depending on satellite zenith angle. For example, at nadir thin cirrus seen by the split-window method corresponds to almost all the cirrus seen by ISCCP, plus some cirrostratus, midlevel clouds and very thin low clouds. Thick and dense cirrus defined by the split-window method almost all fall into the cirrostratus category defined by ISCCP. However, as satellite zenith angle increases, the two methods agree better on cirrus. Therefore, Fig. 6 provides the basis for comparing cirrus retrieved by ISCCP and the split-window method as will be shown in the next section.

c. Comparison of retrieved cloud information

For each pixel in the ISCCP DX dataset, the clear-sky TBB and BTD, and the cloudy/clear decision already inferred by the analysis are used by the split-window method to retrieve clouds from the cloudy-sky radiances. We compare the two cloud retrieval techniques by showing cloud-type frequency distributions of each cloud type classified by one technique as a function of the classification by the other. The resulting table is like a two-dimensional probability density function. Five years of data have been processed: results are similar for all years. We show the tables derived from two regions where cirrus clouds prevail: warm pool ocean (western Pacific) and African tropical land (see Tables 1 and 2). Numbers in the tables represent the cloud amount (CA) frequency distribution.

In the warm pool area, both methods identify about
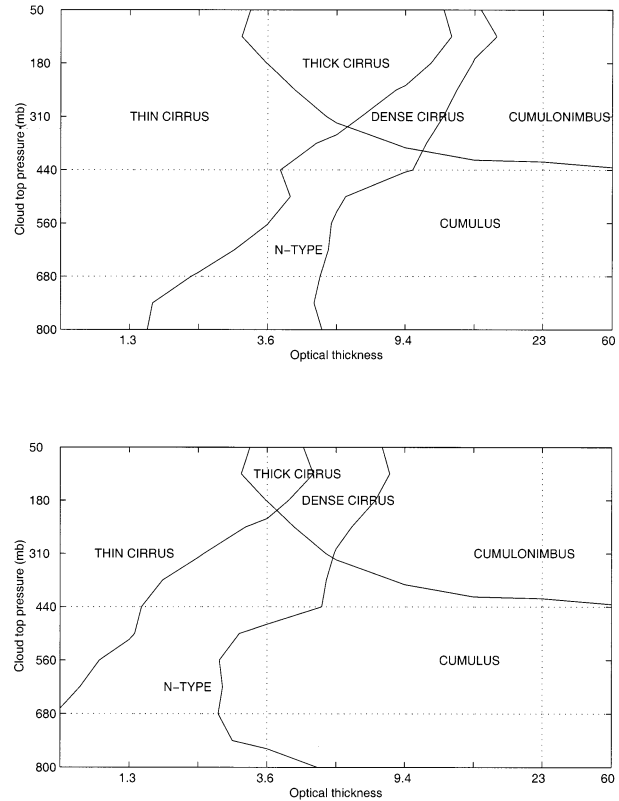
FIG. 6. Simulation of cloud types classified by the split-window method in the Pc–Tau space. (top) Nadir viewing geometry; (bottom) 60° satellite zenith angle. Dashed lines correspond to the ISCCP cloud classification (see Fig. 2).

20%–30% cirrus; however, they do not agree exactly on which clouds are cirrus. More than half of the cirrus clouds identified by the split-window method are called cirrus by ISCCP and the rest are distributed between mid- and low-level thin clouds. A similar distribution is obtained, when surface observations are used to identify cirrus for corresponding ISCCP scenes (Hahn et al. 2001). Likewise, more than three-fourths of cirrus identified by ISCCP are called cirrus by the split-window method, but some are classified as other clouds such as N-type (partial cloud cover, nonblack low-level clouds, and low-level black clouds overlaid by thin cirrus) and cumulonimbus clouds by the split-window method. Over African tropical land, similar results are found, except that both methods find less cirrus there than over the warm pool ocean.

The radiative model studies in the previous section have shown that the cirrus defined by the split-window method may include some optically thin, liquid, midlevel clouds. ISCCP also retrieves cloud-top temperatures that are too large when cirrus overlies lower-level clouds, thus mistakenly labeling some cirrus as altocumulus (Jin et al. 1996; Stubenrauch et al. 1999c). It is hard to tell which effect dominates, based only on the data we have. Further work is needed to separate

TABLE 1. Cloud amount distribution of each cloud type classified by the ISCCP (horizontal) as a function of the classification by the split-window method (vertical). The table is for warm pool oceanic areas; the top half is data for Jan 1990, the bottom half for Jul 1990. Note that sometimes the total cloud amound is different from the sum of the corresponding row or column by about 1, because we round every cloud amount (which is a real number) to an integer and also do the same to the total cloud amount.

	thin ci	thick ci	cirro-stratus	deep con-vection	alto-cumulus	alto-stratus	nimbo-stratus	cumulus	strato-cumulus	stratus	clear	total
					Warm pool ocean: 15°S–15°N, 100°–150°E							
thin ci	11	4	0	0	8	2	0	3	1	0	0	29
thick ci	0	4	1	0	0	0	0	0	0	0	0	5
dense ci	0	3	2	0	0	0	0	0	0	0	0	5
N-type	1	1	0	0	1	3	0	2	2	0	0	10
cumulo-nimbus	0	2	15	8	0	0	0	0	0	0	0	24
cumulus	0	0	0	0	0	1	0	0	1	0	0	4
clear	0	0	0	0	0	0	0	0	0	0	23	23
total	12	14	18	8	9	7	1	5	4	0	23	100

	thin ci	thick ci	cirro-stratus	deep con-vection	alto-cumulus	alto-stratus	nimbo-stratus	cumulus	strato-cumulus	stratus	clear	total
					Warm pool ocean: 15°S–15°N, 100°–150°E							
thin ci	11	3	0	0	5	1	0	3	1	0	0	23
thick ci	0	3	0	0	0	0	0	0	0	0	0	3
dense ci	0	2	1	0	0	0	0	0	0	0	0	3
N-type	1	1	0	0	1	2	0	2	2	0	0	9
cumulo-nimbus	0	2	10	5	0	0	0	0	0	0	0	17
cumulus	0	0	0	0	0	2	0	1	2	0	0	6
clear	0	0	0	0	0	0	0	0	0	0	40	40
total	12	10	11	5	6	5	0	6	5	0	40	100

clouds that are falsely detected as altocumulus by ISCCP from those that are real altocumulus. One possible way might be to make use of collocated radiance data at other wavelengths, such as the 6.7-μm water vapor band, to check the signature of real cirrus, since radiances at 6.7 μm saturate for midlevel clouds but are still sensitive to cirrus.

4. Application to the Mt. Pinatubo case

We make use of the differences of the several cloud retrieval algorithms to find out whether the Mt. Pinatubo volcano eruption affected cirrus.

In the ISCCP analysis, the 0.6-μm visible channel, which is important in determining cloud optical thickness, is also sensitive to scattering by atmospheric aerosols, especially when their optical thickness is larger than normal like following the Mt. Pinatubo eruption. However, aerosol effects are not included in the ISCCP radiative model. Therefore, they will affect the analysis of clouds (Rossow et al. 1996). This effect is negligible in normal conditions when the optical thickness of stratospheric aerosol is of the order 10^{-2}. However, after the large volcanic eruption of Mt. Pinatubo in June 1991, the situation was very different: by late 1991 the stratospheric aerosol optical thickness (at 0.5-μm wavelength) determined from the Stratospheric Aerosol and Gas Experiment (SAGE II) over the equatorial region was around 0.2 or larger, while the value inferred from AVHRR was as large as 0.45 (Stenchikov et al. 1998). An optical thickness of 0.2 is already large enough to

affect the retrieval of thin cirrus in the ISCCP analysis as we show later. The split-window method, on the other hand, is not as easily affected by stratospheric aerosols since it utilizes the radiances from two much longer infrared wavelengths, which are not scattered and absorbed effectively by the very small stratospheric particles. We also examine the 3I cloud data which, like the split-window method, utilizes only IR radiances for cloud property retrieval (there is one cloud test out of eight during daytime that uses visible radiances).

a. "Pinatubo-cirrus" story and one apparent discrepancy

Jensen et al. (1992) studied the possibility that volcanic aerosols may significantly alter the concentration of ice crystals that nucleate in cirrus and assessed the potential impact of these processes on the evolution and radiative properties of cirrus. Their model simulations suggest that under certain conditions the effect on cirrus, of volcanic sulfate aerosols transported down into the upper troposphere, could be to increase the concentration of ice crystals by as much as a factor of 5 and increase the surface warming due to certain types of cirrus near the tropopause by as much as 8 W m^{-2}. Nevertheless, Jensen et al. (1994) found that cirrus properties are generally much less sensitive to the number of condensation nuclei (CN) present than to other factors such as temperature, cooling rate, and vertical wind speed.

Sassen (1992) and Sassen et al. (1995) studied a jet

TABLE 2. The same as Table 1, except for African tropical land.

	thin ci	thick ci	cirro-stratus	deep con-vection	alto-cumulus	alto-stratus	nimbo-stratus	cumulus	strato-cumulus	stratus	clear	total
	African tropical land: 15°S–0°N, 10°–50°E											
thin ci	6	1	0	0	5	1	0	3	1	0	0	17
thick ci	0	1	0	0	0	0	0	0	0	0	0	2
dense ci	0	3	1	0	0	0	0	0	0	0	0	4
N-type	4	1	0	0	4	6	0	4	4	0	0	22
cumulo-nimbus	0	2	14	9	0	0	0	0	0	0	0	25
cumulus	0	0	0	0	0	4	2	0	0	0	0	7
clear	0	0	0	0	0	0	0	0	0	0	23	23
total	10	8	16	9	9	10	2	7	5	0	23	100

African tropical land: 15°S–0°N, 10°–50°E

	thin ci	thick ci	cirro-stratus	deep con-vection	alto-cumulus	alto-stratus	nimbo-stratus	cumulus	strato-cumulus	stratus	clear	total
thin ci	5	0	0	0	5	1	0	4	3	0	0	18
thick ci	0	0	0	0	0	0	0	0	0	0	0	1
dense ci	0	0	0	0	0	0	0	0	0	0	0	0
N-type	1	0	0	0	1	1	0	1	2	0	0	7
cumulo-nimbus	0	0	1	0	0	0	0	0	0	0	0	2
cumulus	2	0	0	0	3	2	2	1	4	0	0	14
clear	0	0	0	0	0	0	0	0	0	0	58	58
total	8	2	1	0	9	5	2	7	9	0	58	100

stream cirrus case during the FIRE II Intensive Field Observations (IFO) and suggested that Pinatubo aerosols might be influencing the cirrus properties. The field observations were carried out in south Kansas on 5 and 6 December 1991 during a period of moist subtropical flow when a strong jet stream swept cirrus clouds through the area. Observed tropopause folding was believed to be the mechanism for injecting stratospheric aerosols of volcanic origin into the troposphere. Unusual cirrus cloud microphysical properties, such as "abnormally high ice crystal concentration, perhaps unique radial ice crystal shapes, and relatively large haze particles in cirrus uncinus," suggested the alteration of cirrus by contamination from decaying volcanic debris within six months of the Mt. Pinatubo volcano eruption (Sassen et al. 1995). They also pointed out the possible climatic implications. Although the Mt. Pinatubo aero-

sol is estimated to have cooled the earth's surface temperature by less than 1°C by direct reflection of incoming solar radiation, the additional effects of perturbed cirrus clouds could provide either a competing or reinforcing climatic perturbations in the years following the eruption.

Wylie and Menzel described a gradual increase of high-level cloud amount in the Tropics and northern midlatitudes by about 0.005 yr^{-1} from 1989 to 1997. They employed a cloud retrieval technique, called the CO_2 slicing method, which is capable of correctly identifying most of transmissive clouds using the HIRS infrared bands with partial CO_2 absorption (Wylie et al. 1994). The CO_2 slicing technique using the HIRS instrument is more sensitive to very thin cirrus than is ISCCP, finding almost twice as much thin cirrus as the first version of ISCCP (C series) found (Jin et al. 1996). A study by Stubenrauch et al. (1999b) shows an improvement of cirrus frequencies by 10%–20% (relative) from CX to the DX version of ISCCP due to increased sensitivity to cirrus over land in the DX analysis and a better treatment of ice clouds in the DX radiative model. On the other hand, the CO_2 slicing technique is sensitive to surface temperature errors. Positive surface temperature errors cause detection of more thin cirrus. Jin et al. (1996) found that in the old HIRS analysis (Wylie et al. 1994) SST values are about 2 K warmer than the blended satellite-ship values, but its surface temperature is significantly underestimated over high topography causing an underdetection of cirrus.

Figure 7 shows the global changes of cirrus detected by ISCCP during a period of 5 years: from January 1989 to December 1993. In contrast with Wylie and Menzel's
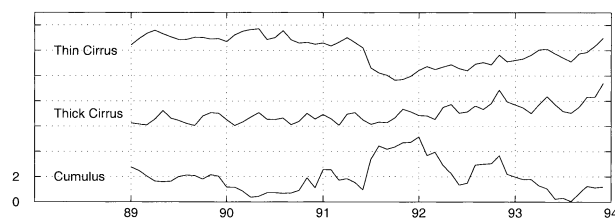
FIG. 7. Deviations of global (excluding polar regions) monthly mean cirrus and cumulus cloud amount derived from the ISCCP. See text (section 4b) for the definition of thin cirrus and thick cirrus. A longer time series can be found in Fig. 7 by Rossow and Shiffer (1999). Only clouds over the ocean are shown. The number on the ordinate gives the magnitude of the cloud amount deviation ×100 (e.g., 2 represents 0.02). Curves are shifted from the each other for better viewing.
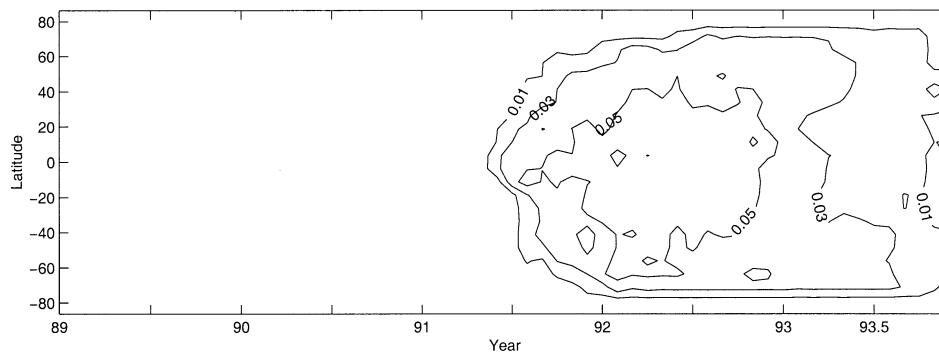
FIG. 8. The evolution of the stratospheric aerosol extinction at 1.02 μm derived from SAGE II, before and after the Mt. Pinatubo eruption in Jun 1991.

and Sassen's findings, ISCCP sees a decrease in thin cirrus (defined below) cloud amount by 0.02–0.04 globally after the eruption of Mt. Pinatubo. However, the corresponding and opposite change of cumulus cloud amounts shown in the same figure, together with the fact that both changes occur preferentially over oceans, suggests that these changes may be caused by the effect of the aerosol in the satellite visible radiances instead of real changes of the clouds (Rossow and Schiffer 1999). Detailed discussions concerning how an aerosol contribution to optical thickness for thin cirrus translates in the ISCCP cloud algorithm to a change of cloud types are given in the next section. During the same period of time, an increase in the average optical thickness of cirrus is also found in the ISCCP dataset, which still might be consistent with Sassen and Jensen's studies.

What actually happened to cirrus after the Mt. Pinatubo eruption? To answer this question, we check other satellite observations that are not as sensitive to volcanic aerosols.

b. The most likely scenario for the changes of cirrus properties after the Mt. Pinatubo volcano eruption

The Mt. Pinatubo volcano erupted on Luzon Island in the Philippines (15.10°N, 120.40°E), with the strongest explosion occurring on 15 June 1991. Following the 15 June eruption, the evolving cloud of water vapor, sulphurous gases, and aerosol spread out both longitudinally and latitudinally and occupied a latitude band of approximately 20°S–30°N within a few months (McCormick et al. 1995). Figure 8 shows the zonal mean total stratospheric aerosol extinction as a function of latitude and time observed from SAGE II (cf. Fig. 3 in Stenchikov et al. 1998). Total stratospheric aerosol extinction at 1.02-μm wavelength was about 0.05 km^{-1} or even higher in tropical and subtropical regions from one or two months after the volcano to around a year and a half later. This is greater than the pre-eruption level by about a factor of 50. Stenchikov et al. (1998) calculated aerosol optical thickness from these data: at 0.525-μm wavelength values exceeded 0.2.

The influence of the volcanic event on the amounts of various cloud types, as seen by ISCCP and the split-window data, are shown in Figs. 9 and 10. These two figures show the zonal mean cloud amount as a function of latitude and time, starting from the beginning of 1989 to the end of 1993. To isolate the influence of the volcano eruption, the mean seasonal cycle has been removed from the original data (seasonality is calculated by averaging all available data for each month and then removing the average from the original data). Similar to the data manipulation in the previous section, each cloudy pixel is processed according to the two cloud retrieval methods and then cloud amount is calculated in a large region by counting the fraction of cloudy pixels. The original ISCCP cirrus cloud classification is further divided into two groups: thin cirrus (Tau < 1.3) and thick cirrus (1.3 < Tau < 3.6). Such a division is justified by their different responses to the volcanic eruption as will be shown. Over tropical and subtropical oceans, ISCCP sees a dramatic decrease of thin cirrus clouds after the Mt. Pinatubo eruption, decreasing from a normal value around 0.1 to below 0.02 and not fully recovering until late 1993. Similar changes are not observed for thin cirrus over land. In the ISCCP dataset, there is also a slight increase in thick cirrus over both ocean and land. On the other hand, observations from the split-window analysis do not show any significant changes of thin or thick cirrus associated with the volcanic eruption over either ocean or land.

Since the optically thinnest, high-level clouds are usually detected by the IR threshold method, aerosols will not significantly affect cloud detections (Rossow and Schiffer 1999). However, because the ISCCP radiative model does not include aerosol effects, any additional reflectance caused by aerosols is combined with that by clouds, thus increasing the retrieved cloud optical thickness. In this situation, the thinnest cirrus may be misclassified as some other type. In the ISCCP analysis, the clear-sky visible reflectance over ocean is constrained by a model of ocean surface reflectance, so that the additional visible reflectance caused by volcanic aerosols is included with the clouds; but over land, the
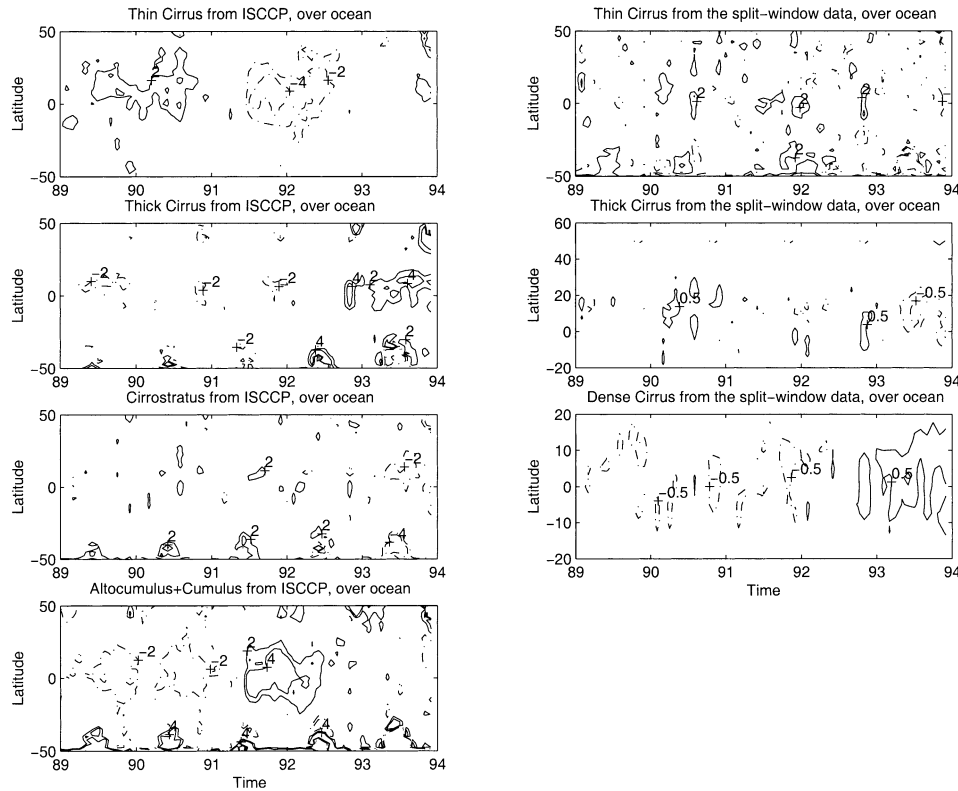
FIG. 9. Zonal mean cloud amount anomalies of various cloud types as a function of latitude and time, derived from the ISCCP and the split-window observations. Only clouds over the ocean are considered. The contour scales are cloud amount anomalies ×100.

clear-sky reflectance is calculated from the data each month, so, the volcanic aerosols increase the land surface visible reflectance and not the clouds (Rossow and Schiffer 1999). Thus, the Pinatubo aerosols increase the ISCCP-retrieved average optical thickness of cirrus over ocean as first pointed out by B. Soden (1997, personal communication). Furthermore, the submicron-sized aerosols have a smaller asymmetry parameter, thus they are better reflectors of incoming solar radiation than the larger cirrus particles. As a result, their contributions to the retrieved cloud optical thickness are even greater than their nominal optical thickness values. All these effects are negligible in normal conditions, but after the Pinatubo event, aerosol layers as thick as 0.2 are comparable to some thin cirrus clouds. In the ISCCP analysis, cloud-top pressure is adjusted for optically thin clouds to account for transmitted IR radiation. This adjustment process is very sensitive to the optical thickness value used for the thinnest clouds; indeed, for those cirrus with optical thickness less than 1, sensitivity tests show that the magnitude of the reflectivity increase by the volcanic aerosol may cause the ISCCP analysis to retrieve cloud-top temperature tens of degrees warmer. Therefore, the extra visible reflectance added to the thin cirrus cloud layers by the Pinatubo aerosols causes the reassignment of thin cirrus to lower-level cloud types. Figure 9 shows an increase of altocumulus and cumulus

clouds in the ISCCP results as expected from this analysis. Moreover, the split-window method, which is not so sensitive to volcanic aerosols, shows little change in thin cirrus amount.

Figure 11 compares the variation of cirrus cloud amount with time from the ISCCP and 3I datasets, covering a few years before and after the Mt. Pinatubo eruption. The observations used in this analysis of the 3I dataset are from the *NOAA-11* satellite; only daytime observations are shown. Again, seasonal cycles are removed from the original data. Generally, thin cirrus (Pc < 440 mb and $N\epsilon_{cld} < 0.5$) and thick cirrus (Pc < 440 mb and $0.5 < N\epsilon_{cld} < 0.9$) as seen by 3I do not show any significant changes that are associated with Mt. Pinatubo eruption. There are some changes of cirrus over tropical and subtropical land, but they are probably caused by the shifting orbit of *NOAA-11,* which has a larger effect on cloud sampling over land where the diurnal cycle of clouds may be stronger. The 3I cloud datasets should, in general, not be affected by the volcanic aerosols due to the use of IR radiances; however, there is one cloud test out of eight during daytime that uses visible radiances. Therefore, the small increase about 0.02 of thin cirrus over subtropical and tropical land is attributable to such an effect (Stubenrauch and Eddounia 2001). Thin cirrus, as seen by ISCCP, decreases dramatically and abruptly in the Tropics (up to
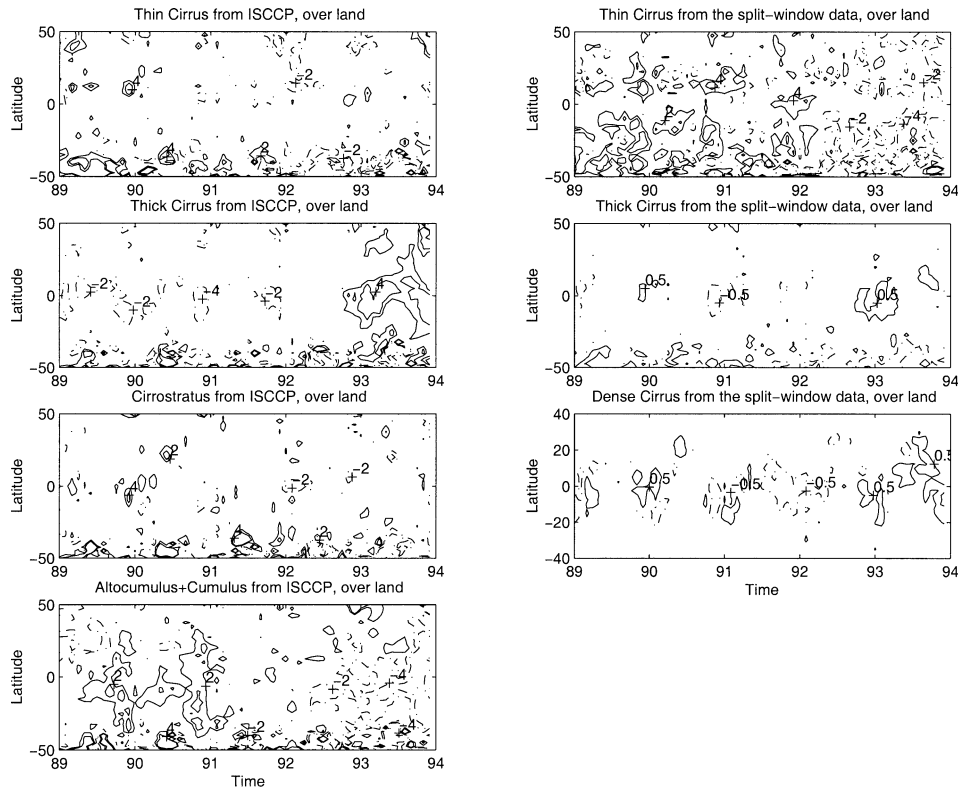
FIG. 10. The same as Fig. 9, except that only clouds over land are considered.

0.08 decrease within a few months) and thick cirrus increases gradually after the Mt. Pinatubo volcanic eruption. So, this comparison shows the same contrast in changes of cirrus after the Mt. Pinatubo eruption as in the ISCCP–split window comparison.

In fact, comparing Fig. 8 with Figs. 9, 10, and 11 provides further support for our interpretation. The aerosol patterns derived from SAGE II and thin cirrus distributions seen by ISCCP are spatially and temporally very similar, with a correlation coefficient as high as -0.85 in the Tropics. In contrast, the correlation between the 3I thin cirrus and the SAGE II aerosol is 0.35 in the same region; the correlation between the thin cirrus identified by the split-window method and the SAGE II is only 0.09. This appears to be consistent with the relative sensitivities of these methods to aerosols.

Besides area coverage, cloud optical thickness (which depends on particle number density and size) is another important cloud property that determines cloud radiative effects. Even if cirrus cloud amount has not undergone significant changes after the Mt. Pinatubo eruption, their microphysical properties (and their optical thickness) may still have been affected by volcanic aerosols. Since the optical thickness reported by ISCCP includes the contribution from aerosols, we use the BTD between 11 and 12 μm as a surrogate. Figures 12 and 13 show the BTD for tropical and subtropical cirruslike clouds identified by both ISCCP and the split-window method

as a function of latitude and time (only tropical and subtropical BTDs are shown because the split-window method works better at lower latitudes than at higher latitudes). Similar to Figs. 9 and 10, the mean seasonal cycle has been removed from the original data. BTD for clear sky is also shown for comparison in Fig. 13. Generally, BTDs for cirrus do not change significantly after the Mt. Pinatubo eruption. (Note that the ISCCP temperature digitization is about 0.5°–0.8° for the temperature range relevant here.) There is a slight increase of BTD for the ISCCP-identified thin cirrus and an opposite tendency for thick cirrus throughout the whole period from 1990 to 1994. According to simulations (see Fig. 3 and 4), this may indicate increasing cloud optical thickness. In other words, both thin and thick cirrus may have thickened slightly. However, caution should be exercised in interpreting these results. First, the magnitude of the changes of BTD for cirrus (about 0.3°–0.6°) is comparable to or even smaller than the temperature digitization step (about 0.5°–0.8°). So, the changes are only marginally detectable, and probably not significant. Second, the pattern of BTD changes did not follow that of the Pinatubo aerosols (see Fig. 8). It looks more like a continuous trend, starting from early 1990. Hence, there may be reasons for this change other than an indirect effect of volcanic aerosols. For example, Wielicki et al. (2002) and Chen et al. (2002) found an increase of outgoing longwave radiation and a decrease of reflected
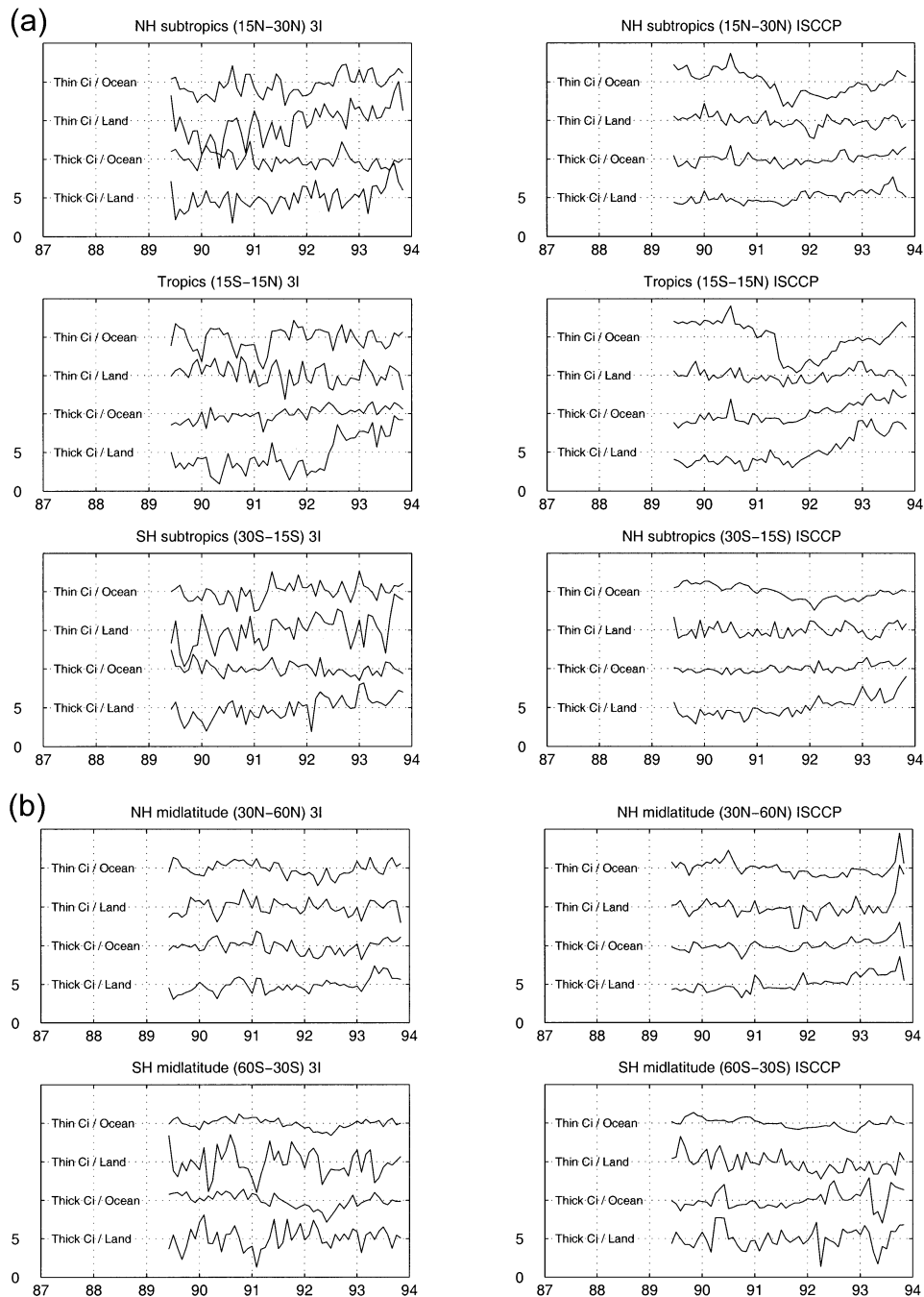
FIG. 11. (a), (b) Cirrus cloud amount anomalies as a function of time from the ISCCP and 3I dataset. The numbers on the ordinate give the magnitude of the cloud amount anomalies ×100 (e.g., 5 represents 0.05). Curves are shifted from each other for better viewing.

sunlight over the period 1985–2000, with most of the increase occurring after 1990. Although these studies do not directly account for the changes of the BTD for cirrus in this study, they illustrate that other decadal-scale changes of the atmosphere and clouds may exist. Therefore, our results are inconclusive in showing any significant influence of the Mt. Pinatubo aerosols on

cirrus optical thickness over the temporal and spatial scales covered by our data. However, this study should not be taken as a contradiction of Sassen et al.'s (1995) results because they looked at changes of cirrus during a particular meteorological event. It is still possible that the Pinatubo aerosols have a local influence on cirrus, like that observed by Sassen et al., but we did not find
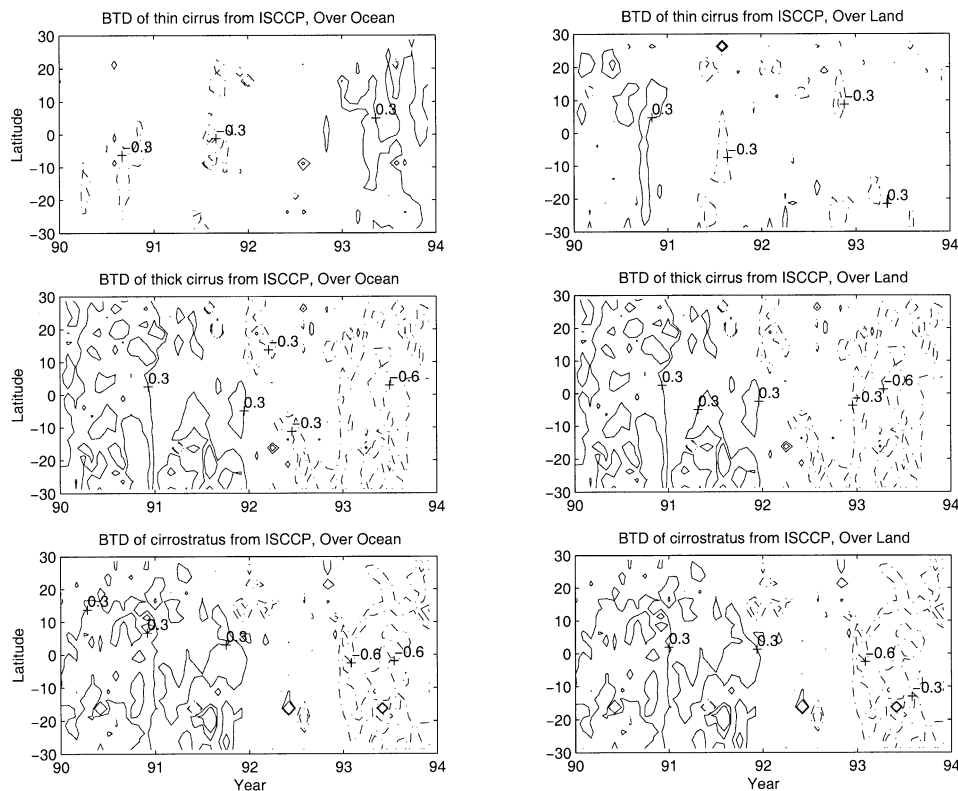
FIG. 12. Zonal mean BTD anomalies as a function of latitude and time, derived from the ISCCP.

any widespread, systematic effect on either cirrus amount or cirrus optical properties.

5. Summary and discussion

In the first half of the paper, we compared cirrus retrieved by ISCCP and the split-window method. By using a radiative transfer model, Streamer, a series of simulations have been carried out, showing that cirrus clouds, defined in ISCCP as $Pc < 440$ mb and $Tau < 3.6$, generally have a large BTD, which is used by the split-window method to isolate cirrus. However, the simulations also show that some thin midlevel clouds with small liquid particles could exhibit BTD values large enough to be included in the thin cirrus category. When applied to AVHRR data, both ISCCP and the split-window method identify around 20%–30% of cirrus clouds in the tropical oceanic and terrestrial regions; however, there is detailed disagreement in classification for half of these clouds (see Fig. 6). These discrepancies are attributed to the different simplifying assumptions made by both methods. For example, the split-window method does not consider water clouds that may show a similar signature as high-level ice clouds. ISCCP, on the other hand, may retrieve a cloud-top temperature that is too large for some cirrus because of small errors in the retrieved optical thickness. Collocated 6.7-μm water vapor channel radiances, which are sensitive to high-level clouds, but not to midlevel clouds, would be helpful in resolving some of these discrepancies.

In the second half of the paper, we make use of different sensitivities of several cloud retrieval techniques to find out what actually happened to cirrus after the Mt. Pinatubo volcanic eruption. The datasets taken into consideration are the ISCCP data, the split-window observations, and 3I cloud data. Because the latter two datasets are derived from infrared radiances, they are much less sensitive to volcanic aerosols than the ISCCP data (although daytime 3I results have some sensitivity to visible reflectivity increase by aerosols). After the Mt. Pinatubo eruption, ISCCP detects a decrease of thin cirrus ($Pc < 440$ mb; $Tau < 1.3$) over ocean, accompanied by a comparable increase of altocumulus and cumulus clouds; over land no significant changes of thin cirrus have been observed in ISCCP. On the contrary, results from the split-window observations and 3I data show little change in thin cirrus that is associated with the volcanic eruption over both ocean and land. Careful examination of ISCCP cloud algorithm suggests that the apparent large decrease of thin cirrus in the ISCCP data is probably an artifact due to the additional visible reflection by volcanic aerosols suspended in the stratosphere (Rossow and Schiffer 1999). This would affect both cloud optical thickness and adjustment of cloud-top height; thus, thin cirrus could be classified as other clouds. Over land, the volcanic aerosols just increase
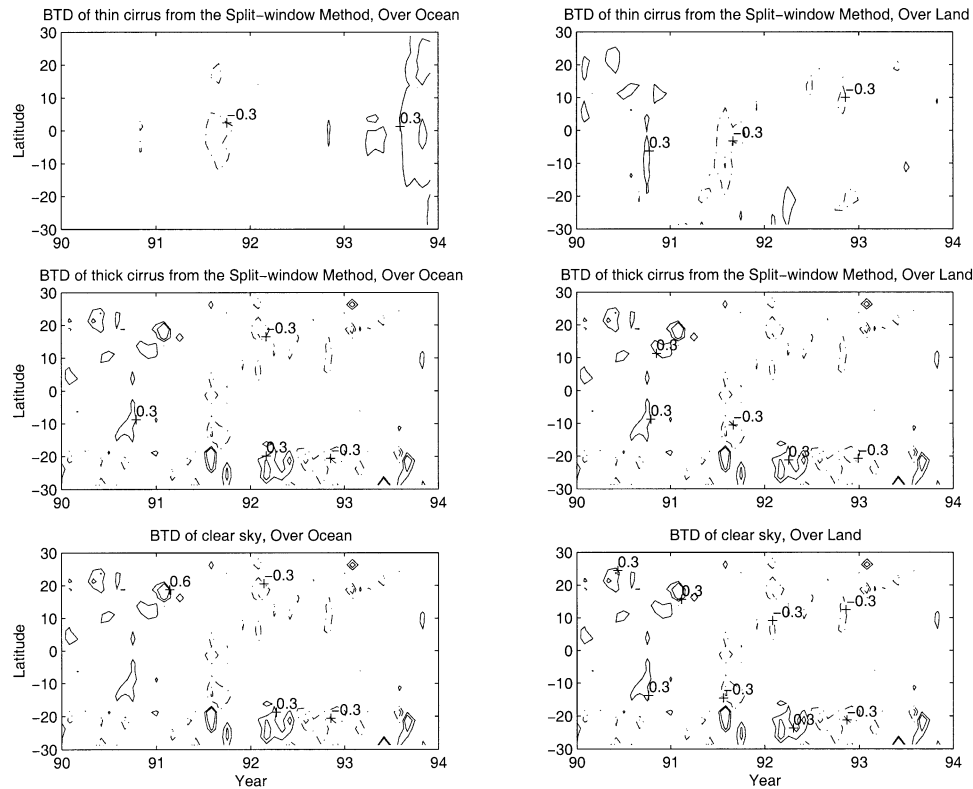
FIG. 13. The same as in Fig. 12, except from the split-window method. Also, BTD for clear sky is shown in the lower panels.

land surface visible reflectance (as found). Therefore, the most likely scenario is close to what has been observed by 3I data and the split-window observations.

Besides cirrus cloud coverage, another possible influence on cirrus of the Mt. Pinatubo volcano eruption is some alteration of cloud microphysical (and optical) properties. However, by looking at the changes of the BTD as a surrogate of cloud optical thickness, it is suggested that the Pinatubo aerosols did not systematically and significantly influence cirrus optical properties on the global scale, either. Previous studies showing some changes are probably isolated local effects. Thus, there is no indication in these results of a climatically significant feedback where aerosol-altered cirrus produced an additional climate effect beyond the direct aerosol-radiative effect.

REFERENCES

Chédin, A., N. A. Scott, C. Wahiche, and P. Moulinier, 1985: The improved initialization inversion method: A high resolution physical method for temperature retrievals from satellites of the TIROS-N series. *J. Climate Appl. Meteor.,* **24,** 128–143.

Chen, J., B. E. Carlson, and A. D. DelGenio, 2002: Evidence for strengthening of the tropical general circulation in the 1990s. *Science,* **295,** 838–841.

Ellingson, R. G., J. Ellis, and S. Fels, 1991: The intercomparison of radiation codes used in climate models: Longwave results. *J. Geophys. Res.,* **96,** 8929–8953.

Fu, Q., and K. N. Liou, 1993: Parameterization of the radiative properties of cirrus clouds. *J. Atmos. Sci.,* **50,** 2008–2025.

Giraud, V., O. Thouron, J. Riedi, and P. Goloub, 2001: Analysis of direct comparison of cloud top temperature and infrared split window signature against independent retrievals of cloud thermodynamic phase. *Geophys. Res. Lett.,* **28,** 983–986.

Hahn, C. J., W. B. Rossow, and S. G. Warren, 2001: ISCCP cloud properties associated with standard cloud types identified in individual surface observations. *J. Climate,* **14,** 11–28.

Hu, Y. X., and K. Stamnes, 1993: An accurate parameterization of the radiative properties of water clouds suitable for use in climate models. *J. Climate,* **6,** 728–742.

Inoue, T., 1985: On the temperature and effect emissivity determination of semitransparent cirrus clouds by bispectral measurements in the 10 μm window region. *J. Meteor. Soc. Japan,* **63,** 88–98.

——, 1987: A cloud type classification with NOAA7 split-window measurements. *J. Geophys. Res.,* **92,** 3991–4000.

——, 1989: Features of clouds over the tropical Pacific during northern hemispheric winter derived from split window measurements. *J. Meteor. Soc. Japan,* **67,** 621–637.

Jensen, E. J., and O. B. Toon, 1992: The potential effects of volcanic aerosols on cirrus cloud microphysics. *Geophys. Res. Lett.,* **19,** 1759–1762.

——, ——, D. L. Westphal, S. Kinne, and A. J. Heymsfield, 1994:

Microphysical modeling of cirrus 2: Sensitivity studies. *J. Geophys. Res.,* **99,** 10 443–10 454.

Jin, Y., and W. B. Rossow, 1997: Detection of cirrus overlapping low-level clouds. *J. Geophys. Res.,* **102,** 1727–1737.

——, ——, and D. P. Wylie, 1996: Comparison of the climatologies of high-level clouds from HIRS and ISCCP. *J. Climate,* **9,** 2850–2879.

Key, J., 1996: Streamer user's guide. Tech. Rep. 96-01, Department of Geography, Boston University, Boston, MA, 91 pp.

Liou, K. N., 1986: Influence of cirrus clouds on weather and climate processes: A global perspective. *Mon. Wea. Rev.,* **114,** 1167–1199.

Liao, X., W. B. Rossow, and D. Rind, 1995: Comparison between SAGE II and ISCCP high-level clouds. Part I: Global and zonal mean cloud amounts. *J. Geophys. Res.,* **100,** 1121–1135.

McClatchey, R. A., R. W. Fenn, J. E. A. Selby, F. E. Volz, and J. S. Garing, 1971: Optical properties of the atmosphere. Air Force Cambridge Research Laboratory Rep. AFCRL-71-0279, Bedford, MA, 85 pp.

McCormick, M. P., L. W. Thomason, and C. R. Trepte, 1995: Atmospheric effects of the Mt. Pinatubo eruption. *Nature,* **373,** 399–404.

Mitchell, D. L., Y. Liu, and A. Macke, 1996: Modeling cirrus clouds. Part II: Treatment of radiative properties. *J. Atmos. Sci.,* **53,** 2967–2988.

Parol, F., J. C. Buriez, G. Brogniez, and Y. Fouquart, 1991: Information content of AVHRR channel 4 and 5 with respect to the effective radius of cirrus cloud particles. *J. Appl. Meteor.,* **30,** 973–984.

Pinto, J. O., J. A. Curry, and C. W. Fairall, 1997: Radiative characteristics of the Arctic atmosphere during spring as inferred from ground-based measurements. *J. Geophys. Res.,* **102,** 6941–6952.

Ramanathan, V., E. J. Pitcher, R. C. Malone, and M. L. Blackmon, 1983: The response of a spectral general circulation model to refinement in radiative process. *J. Atmos. Sci.,* **40,** 605–630.

Randall, D. A., Harshvardhan, D. A. Dazlich, and T. G. Corsetti, 1989: Interactions among radiation, convection, and large-scale dynamics in a general circulation model. *J. Atmos. Sci.,* **46,** 1943–1970.

Rossow, W. B., 1989: Measuring cloud properties from space: A review. *J. Climate,* **2,** 201–213.

——, and R. A. Schiffer, 1991: ISCCP cloud data products. *Bull. Amer. Meteor. Soc.,* **72,** 2–20.

——, and L. C. Garder, 1993: Cloud detection using satellite measurements of infrared and visible radiances for ISCCP. *J. Climate,* **6,** 2341–2369.

——, and ——, 1999: Advances in understanding clouds from ISCCP. *Bull. Amer. Meteor. Soc.,* **80,** 2261–2287.

——, A. W. Walker, D. Beuschel, and M. Roiter, 1996: International Satellite Cloud Climatology Project (ISCCP) description of new cloud datasets. WMO Tech. Doc. 737, World Climate Research Programme (ICSU and WMO), 115 pp.

Sassen, K., 1992: Evidence for liquid-phase cirrus cloud formation from volcanic aerosols: Climatic implications. *Science,* **257,** 516–519.

——, and Coauthors, 1995: The 5–6 December 1991 FIRE IFO II jet stream cirrus case study: Possible influences of volcanic aerosols. *J. Atmos. Sci.,* **52,** 97–123.

Schiffer, R. A., and W. B. Rossow, 1983: The International Satellite Cloud Climatology Project (ISCCP): The first project of the World Climate Research Programme. *Bull. Amer. Meteor. Soc.,* **64,** 779–784.

Song, N., D. O. Starr, D. J. Wuebbles, A. Williams, and S. M. Larson, 1996: Volcanic aerosols and interannual variation of high clouds. *Geophys. Res. Lett.,* **23,** 2657–2660.

Stamnes, K., S. C. Tsay, W. Wiscombe, and K. Jayaweera, 1988: Numerically stable algorithm for discrete-ordinate-method radiative transfer in multiple scattering and emitting layered media. *Appl. Opt.,* **27,** 2502–2509.

Stenchikov, G. L., I. Kirchner, A. Robock, H.-F. Graf, J. C. Antuna, R. G. Grainger, A. Lambert, and L. Thomason, 1998: Radiative forcing from the 1991 Mount Pinatubo volcanic eruption. *J. Geophys. Res.,* **103,** 13 837–13 857.

Stephens, G. L., S.-C. Tsay, P. W. Stackhouse Jr., and P. J. Flatau, 1990: The relevance of the microphysical and radiative properties of cirrus clouds to climate and climate feedbacks. *J. Atmos. Sci.,* **47,** 1742–1754.

Stubenrauch, C. J., and F. Eddounia, 2001: Cloud property survey from satellite observations using vertical sounders (TOVS Path-B) and imagers (ISCCP). *Proc. Workshop on Ion–Aerosol–Cloud Interaction,* Geneva, Switzerland, CERN, 63–74.

——, N. A. Scott, and A. Chedin, 1996: Cloud field identification for earth radiation budget studies. Part I: Cloud field classification using HIRS-MSU sounder measurements. *J. Appl. Meteor.,* **35,** 416–427.

——, A. Chédin, R. Armante, and N. A. Scott, 1999a: Clouds as seen by satellite sounders (3I) and imagers (ISCCP). Part II: A new approach for cloud parameter determination in the 3I algorithms. *J. Climate,* **12,** 2214–2223.

——, W. B. Rossow, F. Cheruy, A. Chédin, and N. A. Scott, 1999b: Clouds as seen by satellite sounders (3I) and imagers (ISCCP). Part I: Evaluation of cloud parameters. *J. Climate,* **12,** 2189–2213.

——, ——, N. A. Scott, and A. Chédin, 1999c: Clouds as seen by satellite sounders (3I) and imagers (ISCCP). Part III: Spatial heterogeneity and radiative effects. *J. Climate,* **12,** 3419–3442.

Wahiche, C., N. A. Scott, and A. Chedin, 1986: Cloud detection and cloud parameters retrieval from the satellites of TIROS-N series. *Ann. Geophys.,* **4B,** 207–222.

Wielicki, B. A., and Coauthors, 2002: Evidence for large decadal variability in the tropical mean radiative energy budget. *Science,* **295,** 841–844.

Wu, M. C., 1987: A method for remote sensing the emissivity, fractional cloud cover, and cloud top temperature of high-level, thin clouds. *J. Climate Appl. Meteor.,* **26,** 225–233.

Wylie, D. P., and W. P. Menzel, 1999: Eight years of high cloud statistics using HIRS. *J. Climate,* **12,** 170–184.

——, ——, H. M. Woolf, and K. I. Strabala, 1994: Four years of global cirrus cloud statistics using HIRS. *J. Climate,* **7,** 1972–1986.